Eur. Phys. J. B (2008)
DOI: 10.1140/epjb/e2008-00054-8

THE EUROPEAN PHYSICAL JOURNAL B

Scaling of the size and temporal occurrence of burst sequences in creep rupture of fiber bundles

Th. Baxevanis[1,a] and Th. Katsaounis[1,2]

[1] Department of Applied Mathematics, University of Crete, Heraklion 714 09, Greece
[2] IACM, FORTH, Heraklion 711 10, Greece

Received 28 September 2007 / Received in final form 10 January 2008
Published online 8 February 2008 –

Abstract. We present a detailed statistical analysis of the size and temporal occurrence of burst sequences in the creep rupture of a proposed *linear* viscoelastic fiber bundle model. According to the model, the burst sequences of fiber breaks display a power law asymptotic behavior analogous to that of the static-fracture [Kloster et al., Phys. Rev. E **56**, 2615, (1997)]. Moreover, power law asymptotics apply to inter-arrival times between successive bursts with a *universal* exponent close to unity.

PACS. 46.35.+z Viscoelasticity, plasticity, viscoplasticity – 46.50.+a Fracture mechanics, fatigue and cracks – 62.20.Mk Fatigue, brittleness, fracture, and cracks

1 Introduction

Materials subjected to a constant load may undergo time-dependent deformation called creep (or "static fatigue"). The underlying creep-damage process is very complex, depended on several characteristics of the specific types of materials, and is far from being well understood. However, experimental studies revealed that the creep behaviors of materials share several universal features. Among these is the power-law statistics behavior of the temporal, spatial and size distribution of acoustic emission (AE) events [1–3], as it is commonly observed in earthquakes [4,5]. Such power-law scaling, observed also in static fracture, implies analogies of material failure with thermodynamic phase transitions and critical phenomena [6], and can be considered indicative of self-similarity in the AE and earthquake source process [7].

Conceptually simple models are an attractive tool for the needs of the above — controversial so far — theoretical problem to embed creep rupture into the general framework of statistical physics. While simple models often fail to reproduce the complex phenomenology observed, they can nevertheless provide meaningful insights. Moreover, qualitative features of such models can be amenable to experimental testing [8]. Thus, the development of simple analytical and numerical models for creep rupture may be of practical importance as well: the development of predictive models can help to identify precursors to failure and rank the severity of damage, so that non-destructive techniques, AE for example, might identify precursor damage prior to failure. Moreover, knowledge of the expected analytic behavior can also guide the extrapolation of data to much longer life situations, usually at lower stresses, than can be tested in acceptable laboratory time scales.

The earliest and simplest models for the stochastic creep-failure process in materials are the classical time-dependent fiber bundle models (FBMs) [9]. FBMs, originally introduced to explain static rupture in heterogeneous materials under tension [10], have been applied to cracks and fractures, earthquakes, and other related breakdown phenomena [11]. FBMs also serve as a starting point for the development of more realistic micromechanical models of the failure of fiber reinforced composites widely used by the modern aerospace and automobile industry. Recently, creep observations have been modeled in terms of novel FBMs with viscoelastic fibers [8,12–14]. An important shortcoming of these models, in contrast to the classical static FBMs [10], is that they do not account for possible burst sequences of fiber breaks as the failure probability remains continuous under step increases in fiber load (although the slope of the failure probability may increase drastically); fibers break one by one. In this respect these models resemble the classical time dependent FBMs. Although the burst avalanches do not relate directly to any experiment, they have been proved of outmost importance in the qualitative description of the fracture process [15].

Here, we start from the models of [12,13] and enrich them with a more realistic rheology in order to account for the classic static bundle feature of instant multiple cracks. Based on the model, we analyze the resulting avalanche size and inter-event times distributions (the inter-event times distribution is affected on average by the avalanche

[a] e-mail: theocharis@tem.uoc.gr

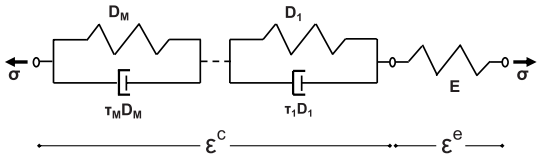

Fig. 1. The proposed Kelvin-Voigt chain rheological model describing the constitutive behavior of the bonds.

size distribution) for the two ends of the load redistribution spectrum, i.e. for global and local load sharing rules. These distributions characterize the fracture process by reflecting the precursory activities (damage accumulation) towards complete fracture. Namely, we describe the rheology of the fibers by the Kelvin-Voigt chain model (Fig. 1). Introduced in the 50's, the Kelvin-Voigt chain model derives naturally from the assumption of *linear* viscoelasticity and is amenable to approximate any linear viscoelastic material to any desired accuracy. We briefly recall its derivation: any linear viscoelastic behavior is described by

$$\varepsilon^t(t) = \int_0^t J(t-t')d\sigma(t'), \tag{1}$$

where the uniaxial compliance function $J(t-t')$ represents the uniaxial strain $\varepsilon^t(t)$ at time t caused by a unit stress — stress is denoted as σ — applied at any time t'. The above integral is a Stieltjes integral in which piece-wise continuous histories $\sigma(t')$ (jumps) are admitted. By approximating the compliance function by a *Dirichlet* series

$$J(t-t') \simeq \frac{1}{E} + \sum_{i=1}^{M} \frac{1}{D_i}\left[1 - \exp\left(-\frac{t-t'}{\tau_i}\right)\right],$$

where τ_i, $i = 1, 2, ...M$, are fixed parameters called retardation times, E is the Young's modulus and D_i, $i = 1, 2, ...M$, are age-independent moduli which can be determined by least-square fitting to the "exact" compliance function, it can be shown that $\varepsilon^t(t) = \varepsilon^e(t) + \varepsilon^c(t) = \varepsilon^e(t) + \sum_{i=1}^{M} \varepsilon_i^c(t)$, where the elastic strain ε^e and creep strains ε_i^c, $i = 1, ...M$, are governed by the following equations

$$\begin{cases} \sigma(t) = E\varepsilon^e(t), \\ \sigma(t) = D_i\varepsilon_i^c(t) + \tau_i D_i \dot{\varepsilon}_i^c(t), \qquad i = 1, 2, ...M. \end{cases} \tag{2}$$

Thus, the approximation of the compliance function by the Dirichlet series corresponds to the Kelvin-Voigt chain in Figure 1 — for further details see [16]. The Kelvin-Voigt chain has been found equivalent to the Maxwell chain model as well as to any other possible rheological (spring-dashpot) model or even to more general models [17].

2 Linear viscoelastic fiber bundle model

The model consists of a 1D linear array of N fibers having the linear viscoelastic constitutive behavior (2), pulled parallel to their direction by an external load. In order to capture failure in the model a strain controlled failure criterion is imposed, i.e. a fiber fails during the time evolution of the system when its total strain exceeds a statistically distributed damage threshold ε^d with probability density $p(\varepsilon^d)$ and cumulative distribution $P(\varepsilon^d) = \int_0^{\varepsilon^d} p(x)dx$.

The simplest approach is to assume global load sharing rule (GLS), i.e. after failure of a fiber its load is transfered equally among the intact fibers, so that the load on fiber i at a certain deformation ε^t is simply given by $\sigma_i(\varepsilon^t) = \sigma(\varepsilon^t)/n_s(\varepsilon^t) = \sigma(\varepsilon^t)/\left[N(1-P(\varepsilon^t)\right]$, where $n_s(\varepsilon^t)$ is the total number of surviving fibers. Thus the macroscopic constitutive equation for the time evolution of the bundle is described by the system

$$\begin{cases} \varepsilon^t(t) = \varepsilon^e(t) + \varepsilon^c(t), \\ \sigma^{ef}(t) = E\varepsilon^e(t), \\ \sigma^{ef}(t) = D_i\varepsilon_i^c(t) + \tau_i D_i \dot{\varepsilon}_i^c(t), \qquad i = 1, 2, .., M, \end{cases} \tag{3}$$

where $\sigma^{ef} = \sigma/[1-P(\varepsilon^t)]$. The proposed time-dependent model reduces to the classical static one in the limit since $J(t-t') \to 1/E$ as $t \to t'$. We restrict our attention to creep rupture, that is to loading paths in which the stress remains fixed to a constant value σ_0. There are two distinct regimes depending on the value of the applied external load σ_0: when σ_0 is below a critical value σ_c then the total strain $\varepsilon^t(t)$ converges asymptotically to a stationary solution ε_s^t, resulting in an infinite lifetime of the composite. This stationary solution ε_s^t can be obtained by setting $\dot{\varepsilon}_i^c = 0$, $i = 1, ..., M$, in (3), i.e. by solving equation $\sigma_0 = \left[1 - P\left(\varepsilon_s^t\right)\right] E\varepsilon_s^t / [1 + E\sum_{i=1}^{M}(1/D_i)]$. The critical stress σ_c is determined from the previous equation as

$$\sigma_c = \frac{1}{1 + E\sum_{i=1}^{M}(1/D_i)}\left[1 - P\left(\varepsilon_c^t\right)\right] E\varepsilon_c^t, \tag{4}$$

where ε_c^t is the solution of $d\left\{\left[1 - P\left(\varepsilon_s^t\right)\right] E\varepsilon_s^t\right\}/d\varepsilon_s^t = 0$. However, if the external load falls above the critical value σ_c then the deformation of the creeping system monotonically increases in time resulting in global failure of the system at a finite time t_f. The creep rupture displacement $\varepsilon_r^t = \varepsilon_r^e + \varepsilon_r^c$ — the total strain at t_f ($\sigma_0 > \sigma_c$) — corresponds to the values of ε^e and ε^c that satisfy

$$\begin{cases} \sigma_0 = \left[1 - P\left(\varepsilon^e + \varepsilon^c\right)\right] E\varepsilon^e = \phi(\varepsilon^e, \varepsilon^c), \\ \partial\phi/\partial\varepsilon^e = 1 - P(\varepsilon^t) - \varepsilon^e p(\varepsilon^t) = 0. \end{cases} \tag{5}$$

Indeed, $d\sigma_0 = (\partial\phi/\partial\varepsilon^e)d\varepsilon^e + (\partial\phi/\partial\varepsilon^c)d\varepsilon^c = 0$ yields $\dot{\varepsilon}^e \to \infty$ for $\partial\phi/\partial\varepsilon^e \to 0$. The above analytical results are justified by direct Monte Carlo simulations of the creeping process for finite systems of N fibers (Fig. 2). In all numerical simulations the viscoelastic behavior of the fibers is described by $M + 1 = 9$ units and the maximum of the retardation times of the different units is denoted as $\tau_M = 10^3$; the retardation times are distributed in a geometric progression with quotient 10, as suggested in [16]. The simulation technique is described in detail in [18].

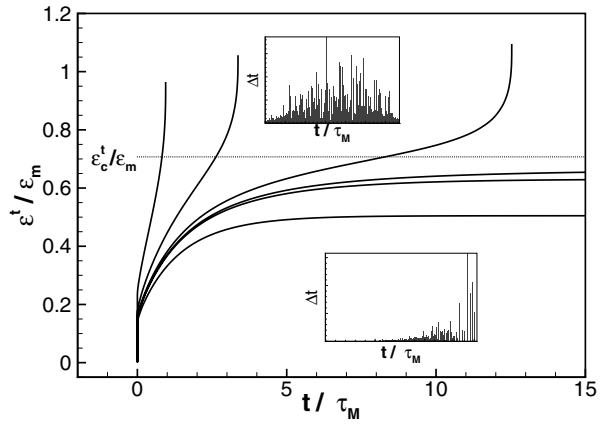

Fig. 2. Total strain $\varepsilon^t(t)$ for several values of σ_0 below and above σ_c (Weibull distribution $P(\varepsilon^d) = 1 - \exp[-(\varepsilon^d/\varepsilon_m)^\alpha]$, $\alpha = 2$) for a bundle of $N = 10^7$ fibers. The critical strain ε_c^t is indicated. The upper inset represents typical values of inter-event times Δt for $\sigma_0 > \sigma_c$ at the time of their occurrence t, while the lower inset is the corresponding plot for $\sigma_0 < \sigma_c$.

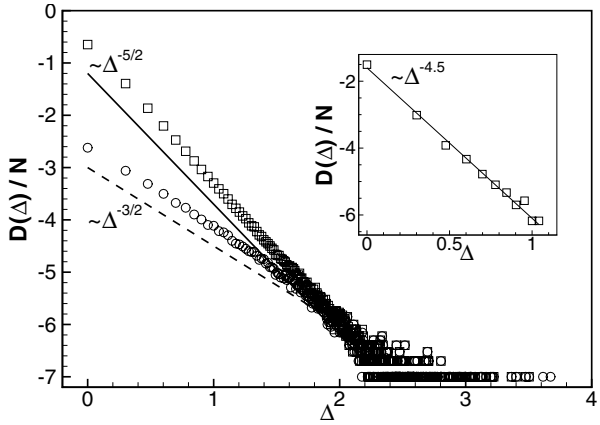

Fig. 3. A log-log plot of the distribution of bursts for GLS (Weibull distribution, $\alpha = 3$) recorded in an interval $(\varepsilon_0^t, \varepsilon_r^t)$, where ε_0^t is the corresponding value of ε^t for $\varepsilon^c = 0$ and $\varepsilon_0^t = 0.9\varepsilon_r^t$ for a bundle of $N = 10^7$ fibers. Inset: The distribution of bursts for LLS (Weibull distribution, $\alpha = 2$). The inset is based on $n = 1000$ samples, each with $N^{'} = 15.000$ fibers ($N = nN^{'}$).

3 Distributions of burst avalanches and times in between successive bursts

Creep is a stress-controlled process, thus the same load must always be endured by the surviving fibers; the same load is simply redistributed. Step load increases following fiber failure — the stresses are assumed to equilibrate infinitely fast (quasistatic assumption) — result in instantaneous increases in elastic strain due to the presence of the degenerate elastic spring in the Kelvin-Voigt chain (Fig. 1). Therefore it is likely that the (total) strain threshold of other non-failed fibers may be exceeded. This mechanism may easily trigger an avalanche. It should be noted that the dynamics of avalanches of fiber breaks is different for the static and the proposed viscoelastic model. Whenever an avalanche stops in the static model, the load of each of the surviving fibers increases so as to become equal to the next stress threshold and then a new avalanche may occur due to the failure of the fiber having this threshold as its strength. In the proposed model however, whenever an avalanche stops, the load of the fibers remains constant until the creep (time-dependent) deformation forces the total deformation to reach the next threshold.

In order to derive analytically the burst distribution $D(\Delta)$ of our model for GLS, consider a small strain per fiber interval $(\varepsilon^t, \varepsilon^t + d\varepsilon^t)$ in a range where the average force σ_0 is constant. For a large number N of fibers the expected number of surviving fibers is $N[1 - P(\varepsilon^t)]$. The thresholds in the interval, of which there are $Np(\varepsilon^t)d\varepsilon^t$, will be Poisson distributed. Assume that time-dependent deformation results in the break of a fiber with threshold ε^t. Then the load that this fiber suffered will be redistributed on the $N[1 - P(\varepsilon^t)]$ remaining fibers. Thus the instantaneous load increase on the surviving fibers will be $d\sigma = E\varepsilon^e/\{N[1 - P(\varepsilon^t)]\}$ which results in a total strain increase $d\varepsilon^t = d\varepsilon^e = \varepsilon^e/\{N[1 - P(\varepsilon^t)]\}$, since the creep strain remains fixed. The average number of fibers that break due to this load increase is

$$\alpha = \alpha(\varepsilon^t; \varepsilon^e) = Np(\varepsilon^t)d\varepsilon^t = \frac{\varepsilon^e p(\varepsilon^t)}{[1 - P(\varepsilon^t)]}.$$

Suppose now that $\sigma_0 > \sigma_c$. Following the analysis in [19], one finds that the distribution of bursts Δ over an interval $(\varepsilon_0^t, \varepsilon_r^t)$ is given by

$$\frac{D(\Delta)}{N} = \frac{\Delta^{\Delta-1}}{\Delta!} \int_{\varepsilon_0^t}^{\varepsilon_r^t} \alpha(\varepsilon^t)^{\Delta-1} e^{-\alpha(\varepsilon^t)\Delta} [1 - \alpha(\varepsilon^t)] p(\varepsilon^t) d\varepsilon^t.$$

For large Δ the maximum contribution comes from the neighborhood of the upper integration limit, since $\alpha(\varepsilon^t)e^{-\alpha(\varepsilon^t)}$ is maximal for $\alpha(\varepsilon^t) = 1$, i.e. for $\varepsilon^t = \varepsilon_r^t$. Expansion around the saddle point yields

$$\frac{D(\Delta)}{N} = C\Delta^{-5/2}\left(1 - e^{-\Delta/\Delta_c}\right), \tag{6}$$

where

$$\Delta_c = 2/[\alpha^{'}(\varepsilon_r^t)^2(\varepsilon_r^t - \varepsilon_0^t)^2], \tag{7}$$

and $C = (2\pi)^{-1/2} p(\varepsilon_r^t)/\alpha^{'}(\varepsilon_r^t)$. Equation (6) yields the asymptotic behavior

$$\frac{D(\Delta)}{N} \propto \begin{cases} \Delta^{-3/2} & \text{for } \Delta \ll \Delta_c, \\ \Delta^{-5/2} & \text{for } \Delta \gg \Delta_c. \end{cases}$$

Such a behavior has been proved in the static global FBMs [19]. The above crossover behavior in burst avalanches is a universal phenomenon, independent of the threshold distribution. The crossover can be used as a sign of imminent failure [20]; the 3/2 power law will occur only when ε_0^t is close enough to the rupture value ε_r^t. Hence, for applications it is important that the 3/2 power law is seen also in a single sample (Fig. 3). In addition, the exact

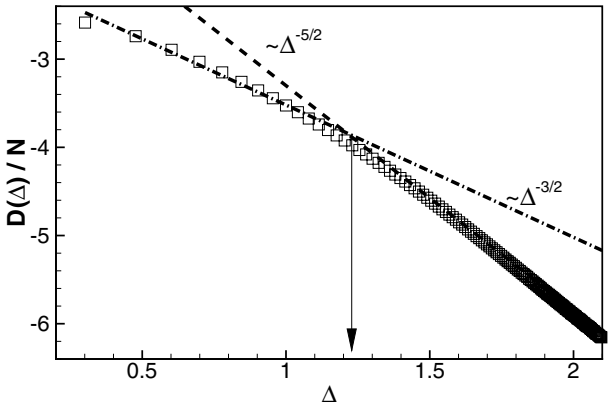

Fig. 4. A log-log plot of the distribution of bursts for the uniform threshold distribution ($P(\varepsilon^d) = \varepsilon^d/\varepsilon_m$) with $\varepsilon_0^t = 0.6\varepsilon_r^t$. The arrow indicates the crossover point. The figure is based on $n = 5 \times 10^4$ samples, each with $N^{'} = 10^6$ fibers ($N = nN^{'}$).

value of the crossover point has been derived (7). For the uniform distribution $\Delta_c = 2(1-\varepsilon_r^t)/[\varepsilon_{r^2}^t(1-\varepsilon_0^t/\varepsilon_r^t)^2]$ (dimensionless values) where $\varepsilon_r^t = 1-\sqrt{\sigma_0}$, so for $\sigma_0 = 0.2$ and $\varepsilon_0^t = 0.6\varepsilon_r^t$ one obtains $\log(\Delta_c) \simeq 1.26$. This value is approximated reasonably well by the numerical example of Figure 4. For local-load sharing rule (LLS), in which the excess load of a bursting fiber is divided equally to the nearest surviving fibers, the model is *not* in the same universality class as the global model. The numerically estimated apparent exponent value for small event sizes is quite larger $\backsimeq$4.5 (the same value 4.5 is found in the static local model [21]) (Fig. 3).

Next, we study the distribution $D(\Delta t)$ of inter-events times Δt between two successive bursts. The inter-event times depend on both the applied load σ_0 and the applied probability distribution. It can be observed in (Fig. 2) that above and below the stationary state (the plateau of ε^t) the inter-event times are relatively sort while along the plateau are scattered over a broad interval. Extensive simulations under GLS revealed that whenever the system attains a macroscopic stationary state, the distribution of inter-event times follows a power law of the form $D(\Delta t) \propto \Delta t^{-\gamma}$ both below and above the critical point (Fig. 5a). The value of the exponent $\gamma = 0.9 \pm 0.05$ is the same on the two sides of the critical stress and it is independent from the disorder distribution. Note, that increasing the load above the critical value σ_c the stationary state gradually disappears, implying that the power law regime preceding the exponential cut-off is getting shorter but the value of γ remains the same. Moreover, a similar exponential decay of the statistical distribution of inter-event times with an exponent $\gamma = 1 \pm 0.05$ was found under LLS independent from the applied load and the failure distribution (Fig. 5b). The empirical value of the exponent γ obtained from experiments was found to depend on the material. Nevertheless, the γ-values reported in literature are in the proximity of unity for both creep [1] and static fracture [22] with the exception of [23].

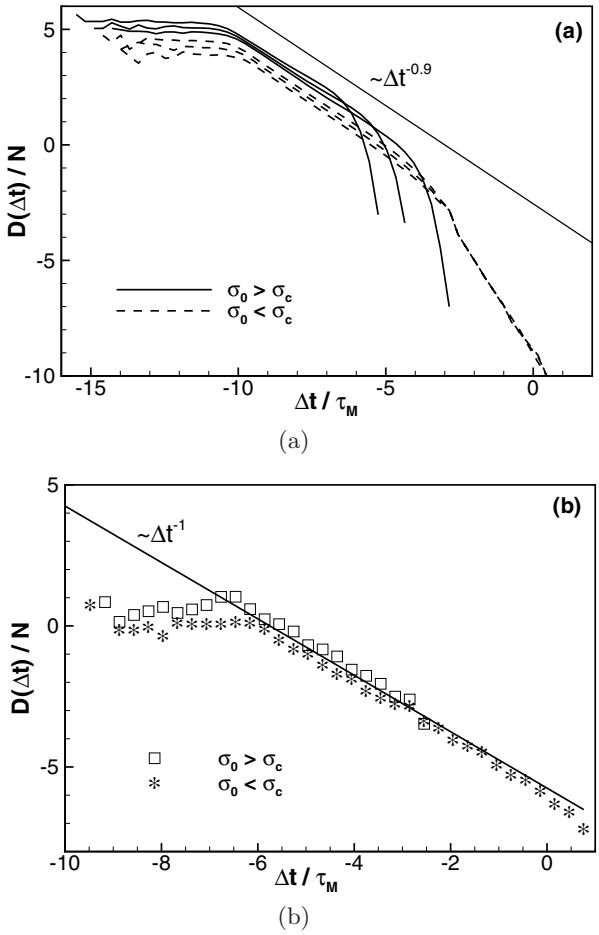

Fig. 5. A log-log plot of the distribution of inter-event times Δt (a) for GLS (Weibull distribution, $\alpha = 4$). The power law behavior can be observed over 5 orders of magnitude (b) for LLS (Weibull distribution, $\alpha = 4$). The power law behavior can be observed over 4 orders of magnitude. The figure is based on $n = 1000$ samples, each with $N^{'} = 15.000$ fibers ($N = nN^{'}$).

The differences between our theoretical results and those in [13,14] on the γ-value are worth mentioning. In contrast to our results, in [13], the exponent γ is not universal; it is different for GLS on the two sides of the critical stress σ_c ($\gamma \simeq 1.5$ for $\sigma_0 > \sigma_c$ and $\gamma \simeq 1.95$ for $\sigma_0 < \sigma_c$, these values were also obtained from a completely different approach of creep failure [14]), while for LLS the system is in the same universality class ($\gamma \simeq 1.9$) as for GLS for stress levels above the critical one. The discrepancy between the latter results and those reported herein are attributed to the influence on inter-event times distributions by the burst avalanches present in our model; in [13,14] fibers break one by one.

4 Conclusions

Concluding, a statistical analysis of the size and temporal occurrence of fracturing events in the creep rupture of a

linear viscoelastic FBM has been presented. In particular, the event sizes and event time-intervals are found to follow a power-law-like statistics. The power-law asymptotic behavior of event sizes is analogous to that of the static-fracture. The observed crossover behavior for GLS can be used as a sign of imminent failure. The power-law exponent derived for the event time-intervals is universal and very close to those obtained in fracturing processes over a wide range of activity. Moreover, the presence of burst avalanches in our model is of importance in its own right due to the applicability of burst sequences in vastly different theoretical studies of the damage-failure process.

References

1. A. Guarino, S. Ciliberto, A. Garcimartín, R. Scorretti, Eur. Phys. J. B **26**, 141 (2002); C. Maes, A. Van Moffaert, H. Frederix, H. Strauven, Phys. Rev. B **57**, 4987 (1998); A. Vespignani, A. Petri, A. Alippi, G. Paparo, Fractals **3**, 839 (1995)
2. J. Davidsen, S. Stanchits, G. Dresen, Phys. Rev. Lett. **98**, 125502 (2007)
3. A. Saichev, D. Sornette, Phys. Rev. E **71**, 016608 (2005)
4. F. Omori, Rep. Earth. Inv. Comm. **2**, 103 (1894) (in Japanese)
5. M. Gutenberg, C.F. Richter, Bull. Seismol. Soc. Amer **34**, 185 (1944)
6. S. Zapperi, P. Ray, H.E. Stanley, A. Vespignani, Phys. Rev. E **59**, 5049 (1999); S. Zapperi, P. Ray, H.E. Stanley, A. Vespignani, Phys. Rev. Lett. **78**, 1408 (1997); J.V. Andersen, D. Sornette, K.-T. Leung, Phys. Rev. Lett. **78**, 2140 (1997)
7. T. Hirata, J. Geophys. Res. **92**, 6215 (1987)
8. H. Nechad, A. Helmstetter, R. El Guerjouma, D. Sornette, Phys. Rev. Lett. **94**, 045501 (2005)
9. B.D. Coleman, J. Appl. Phys. **29**, 968 (1958)
10. H. Daniels, Proc. Royal Soc. A **183**, 405 (1945)
11. *Statistical Models for the Fracture of Disordered Media*, edited by H.J. Herrmann and S. Roux (North-Holland, Amsterdam, 1990); *Modelling Critical and Catastrophic Phenomena in Geoscience*, edited by P. Bhattacharyya, B.K. Chakrabarti (Springer-Verlag, Heidelberg, 2006)
12. R.C. Hidalgo, F. Kun, H.J. Herrmann, Phys. Rev. E **65**, 032502 (2002); F. Kun, R.C. Hidalgo, H.J. Herrmann, K.F. Pál, Phys. Rev. E **67**, 061802 (2003)
13. F. Kun, Y. Moreno, R.C. Hidalgo, H.J. Herrmann, Europhys. Lett. **63**, 347 (2003)
14. R.C. Hidalgo, F.C. Kun, H.J. Herrmann, Physica A **347**, 402 (2005)
15. A. Delaplace, S. Roux, G. Pijaudier-Cabot, J. Engng. Mech. **127**, 646 (2001); T. Baxevanis, F. Dufour, G. Pijaudier-Cabot, Int. J. Frac. **141**, 561 (2006); S. Roux, A. Delaplace, G. Pijaudier-Cabot, Physica A **270**, 35 (1999)
16. M. Jirásek, Z.P. Bažant, *Inelastic Analysis of Structures*. (John Wiley and Sons Ltd, Sussex, 2002)
17. A.J. Staverman, P. Schwarzl, Proc. Acad. Sc., The Netherlands **55**, 486 (1952); M.A. Biot, J. Appl. Phys. **25**, 1385 (1954); Z.P. Bažant, C. Huet, Int. J. Solids Struct. **36**, 3993 (1999)
18. T. Baxevanis, T. Katsaounis, Phys. Rev. E **75**, 046104 (2007)
19. M. Kloster, A. Hansen, P.C. Hemmer, Phys. Rev. E **56**, 2615 (1997)
20. S. Pradhan, A. Hansen, P.C. Hemmer, Phys. Rev. Lett. **95**, 125501 (2005)
21. A. Hansen, P.C. Hemmer, Phys. Lett. A **184**, 394 (1994)
22. L.I. Salminen, A.I. Tolvanen, M.J. Alava, Phys. Rev. Lett. **89**, 185503 (2002)
23. A. Guarino, A. Garcimartín, S. Ciliberto, Eur. Phys. J. B **6**, 13 (1998)